Journal of Magnetism and Magnetic Materials 476 (2019) 387–391

Contents lists available at ScienceDirect

Journal of Magnetism and Magnetic Materials

journal homepage: www.elsevier.com/locate/jmmm

Research articles

Tunable magnetic properties of Ni-doped $CoFe_2O_4$ nanoparticles prepared by the sol–gel citrate self-combustion method

Alexander Omelyanchik[a,*], Gurvinder Singh[b], Mikhail Volochaev[c,d], Alexey Sokolov[c,d], Valeria Rodionova[a,e], Davide Peddis[f,g]

[a] Immanuel Kant Baltic Federal University, Kaliningrad, Russia
[b] Department of Materials Engineering, Norwegian University of Science and Technology (NTNU), Trondheim, Norway
[c] Kirensky Institute of Physics, Federal Research Center KSC SB RAS, Krasnoyarsk, Russia
[d] Siberian Federal University, Krasnoyarsk, Russia
[e] National University of Science and Technology MISiS, Moscow, Russia
[f] Istituto di Struttura della Materia – CNR, Monterotondo Scalo, RM, Italy
[g] Department of Chemistry and Industrial Chemistry (DCIC), Università of Genova, Genova, Italia

ARTICLE INFO

Keywords:
Ferrites materials
Mixed ferrites
Nanostructured materials
Magnetic properties

ABSTRACT

The nanostructured spinel ferrites with complex stoichiometry are an important family of the materials in a number of applications, especially in electronics through their good electrical and magnetic properties. In the framework of this study, a set of mixed cobalt and nickel ferrites was prepared with the sol–gel self-combustion route. The structural and morphological features of particles were studied with X-ray diffraction (XRD), Scanning Transmission Electron Microscopy (STEM) and Energy Dispersive X-ray analysis (EDX) techniques. The prepared particles show a crystalline nature with a monotonic distribution of the elements and particles size distribution in the range of 17–29 nm. The obtained particles demonstrate good magnetic properties with tunable saturation magnetization and magnetic anisotropy, i.e., coercivity depending on chemical composition.

1. Introduction

Owing to the good magnetic and electric properties such as high electrical resistivity and high magnetization saturation, spinel ferrites is a widely-used family of materials that have many applications in energy, electronics, microwave, absorption [1–5]. A general formula of spinel ferrite is $MeFe_2O_4$, where Me is some divalent cation or a combination of several cations (Fe^{2+}, Co^{2+}, Ni^{2+}, Cu^{2+}, Zn^{2+}, …). A typical crystal structure of a spinel is an assembly of two sublattices: octahedral (B) cationic site and tetrahedral (A) cationic site. The super-exchange interaction (Me–O–Me) is responsible for the anti-ferromagnetic order between magnetic cations located in the A and B interstitial sites. The net magnetization originates from the difference in magnetic moments of these sublattices: $M = \Sigma M_{B\text{-site}} - \Sigma M_{A\text{-site}}$. Consequently, the magnetic properties can be controlled by replacing the substituted cations with a different single-atom magnetic moment in various stoichiometries [6,7]. Here Co^{2+} ($3\mu_B$) and Ni^{2+} ($2\mu_B$) are of greatest interest because $CoFe_2O_4$ has stronger cubic magnetocrystalline anisotropy among ferrites ([8]) while Ni^{2+} allows improving electrical properties ([9]) and to tune anisotropy to the lower value for applications' requirements [10–13]. Nickel and cobalt ferrites are an inverted spinel, which means that generally all Fe^{3+} ions are equally distributed in two sites and hence mutually compensated while the net magnetization comes from Me^{2+} ions occupying the octahedral site. However, in a real system, especially in nanostructured materials, a non-equilibrium cations distribution between the spinel's sublattices was observed, which may induce a significant change in anisotropy and magnetization of material [14].

Nanostructure spinel ferrites have interesting electrical and magnetic properties ([4]), as well as a high surface-to-volume ratio, which makes them more attractive in the field of sensors, catalysis, and biomedicine [15–18]. The small size of magnetic nanoparticles (MNPs) leads firstly to the growth of coercivity, reaching a maximum at critical diameters of ~70 and ~100 nm for $CoFe_2O_4$ and $NiFe_2O_4$, respectively and then reduction due to superparamagnetic relaxations [17]. Many attempts have been made to synthesize Co-Ni ferrite MNPs: co-precipitations method [12,19–21]; carbamide/glucose combustion route [11]; polyol method [13]; hydrothermal method [10]; solvothermal method [22], etc. Nonetheless, the development of a cheap and high-throughput process for the production of single-phase spinel ferrite

* Corresponding author.
E-mail address: asomelyanchik@kantiana.ru (A. Omelyanchik).

https://doi.org/10.1016/j.jmmm.2018.12.064
Received 31 August 2018; Received in revised form 3 December 2018; Accepted 15 December 2018
Available online 17 December 2018
0304-8853/

MNPs with a controllable grain size distribution is still in attracting the great attention because the parameters of synthesis, for example, the pH, the temperature and the precursors drastically affect the magnetic properties of ferrites [20,23,24].

Earlier, it was demonstrated that the non-magnetic Zn^{2+} ($0\mu_B$) ions doping of cobalt ferrite can occupy the tetrahedral site, replacing the position of Fe^{3+}. In this case, the Fe^{3+} ions are no longer compensated and contribute to the total magnetic moment; as a result, the saturation magnetization at 5 K reached a high value up to 157 ± 3 A m^2/kg for $Zn_{0.46}Co_{0.54}Fe_{2.02}O_4$ in respect to the value of 109 ± 3 A m^2/kg for the stoichiometric cobalt ferrite [7]. This effect depends on the sizes of the grains and on the method of material synthesis [2,14]. In addition, an increase of magnetization saturation was observed for $Ni_{0.2}Co_{0.8}Fe_2O_4$ and $Ni_{0.4}Co_{0.6}Fe_2O_4$ together with a non-regular dependence of the coercivity [10]. It is worth noting that the size of particles varies significantly, which makes an interpretation of results difficult. G. Muscas and co-workers [13] observed the regular reduction of both saturation magnetization and coercivity field with an increase of nickel content for the Co-Ni ferrite MNPs with a narrow size distribution. The observed behavior is strongly related to an interplay of cations' distribution and spin canting, which was confirmed by Mössbauer spectroscopy performed under an intense magnetic field. Nonhomogenous filling of sublattices, namely the overpopulation of octahedral sites, led to a very high value of saturation magnetization of about 130 ± 10 A m^2/kg at 5 K. This point presents fundamental importance for development of new materials, because the magnetic properties of ferrites can be engineered by the tuning of chemical composition, although this requires a complex investigation of structural and magnetic properties. In this work, a simple and low-cost sol–gel self-combustion method has been used to prepare the set of MNPs of cobalt ferrites with different Ni^{2+} content in the range of 0–100%. This method is a simple one-step route for ferrite powder synthesis with a good crystalline nature without the need for further annealing; in addition, a large amount of product can be obtained, making this synthetic approach interesting for industrial applications [2,18,25].

2. Materials and methods

2.1. Nanoparticles preparation

Samples of MNPs were prepared by the self-combustion method described in detail elsewhere [25]. The metal salts $Fe(NO_3)_3{\cdot}9H_2O$ (Carlo Erba Reagenti SpA 100%), $Co(NO_3)_2{\cdot}6H_2O$ (Scharlab S.L. 98%), and $Ni(NO_3)_2{\cdot}6H_2O$ (Carlo Erba Reagenti SpA 100%) were mixed with the molar ratio to establish the stoichiometry of spinel ferrite $Ni_xCo_{1-x}Fe_2O_4$ with × = 0, 0.25, 0.5, 0.75 and 1. The citric acid (Scharlab S.L. 99.5%) was added to aqueous solutions of prepared mixtures in molar ratio 1:1 to metal salts. The pH-level was adjusted to the value of 7 by dropwise adding of 30% ammonia solution (Carlo Erba Reagenti SpA). Under magnetic stirring at 150 °C, the sol was dried to the gel condition and in about 60 min the temperature of 300 °C was set to induce the self-combustion reaction producing a black-brown "tree-like" structure. The resulting powders were collected and labeled as N_{100}, $N_{75}C_{25}$, $N_{50}C_{50}$, $N_{25}C_{75}$ and C_{100} according to nickel/cobalt content in $Ni_xCo_{1-x}Fe_2O_4$.

2.2. Magnetic and structure properties

The X-ray diffraction (XRD) studies were performed with a Bruker DaVinci2 diffractometer using Cu Kα (λ = 1.54056 Å) in the 2θ geometry in the range of 10–75°. The elemental analysis was carried out with a scanning transmission electron microscopy with X-ray spectroscopy detector option (STEM-EDX, Hitachi TM 3000). The morphology of the samples was investigated with scanning electron microscopy (SEM) with a JEOL JEM-2100 electron microscope operating at 30 kV. The dc magnetic properties were measured with a VSM magnetometer (7400 System Vibrating Sample Magnetometer, Lake Shore Cryotronics Inc.) in the field range up to 1.1 T at room temperature (295 K). To prevent any movement of the powder samples during the measurements, the powder was fixed in an aluminum sample holder with a negligibly small magnetic signal. M − H hysteresis loops were recorded in continuous mode, where 225 points were collected with a time of measurement of 10 s. Because the maximum field is not sufficient to fully saturate the sample, magnetization saturation was extrapolated with the fitting of the high-field region using the Law of Approach to Saturation (LAS) [13,26]: $M(H) = M_S(1–A/H–B/H^2)$, where A and B are fitting parameters. The direct current demagnetization protocol was involved to study irreversible magnetization processes, for that the magnetization at zero field (M_{DCD}) was used after application of gradually increasing field H_{rev} to the sample previously saturated in the opposite direction [13,26].

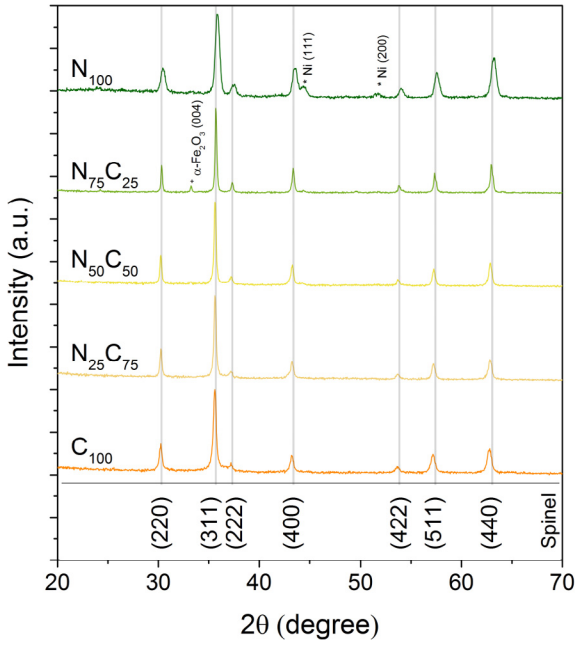

Fig. 1. XRD patterns of mixed ferrite powders. Positions of Bragg peaks are illustrated with lines for cubic spinel, "+" for hematite and "*" for metallic nickel.

Table 1
Chemical composition and microstructural properties of $Ni_xCo_{1-x}Fe_2O_4$ with × = 0, 0.25, 0.5, 0.75 and 1. Crystallite size (d_{XRD}) were calculated with Scherrer's equation on the (4 4 0) peak. Uncertainties in the last figure are given in brackets.

Sample	Composition	d_{XRD}, nm
C_{100}	$CoFe_2O_4$	17(2)
N_{25} C_{75}	$Ni_{0.25}Co_{0.75}Fe_2O_4$	29(3)
N_{50} C_{50}	$Ni_{0.50}Co_{0.50}Fe_2O_4$	25(3)
N_{75} C_{25}	$Ni_{0.75}Co_{0.25}Fe_2O_4$	23(3)
N_{100}	$NiFe_2O_4$	20(2)

3. Results and discussion

3.1. Characterization of nanoparticles

The XRD-spectra of the samples indicated the high crystallinity of the nanoparticles without any amorphous content (Fig. 1). The main diffraction peaks were indexed to a cubic spinel lattice according to PDF cards 22–1085 and 44–1485 for cobalt and nickel ferrite, respectively. Obviously, the positions of the main peaks are equivalent for both

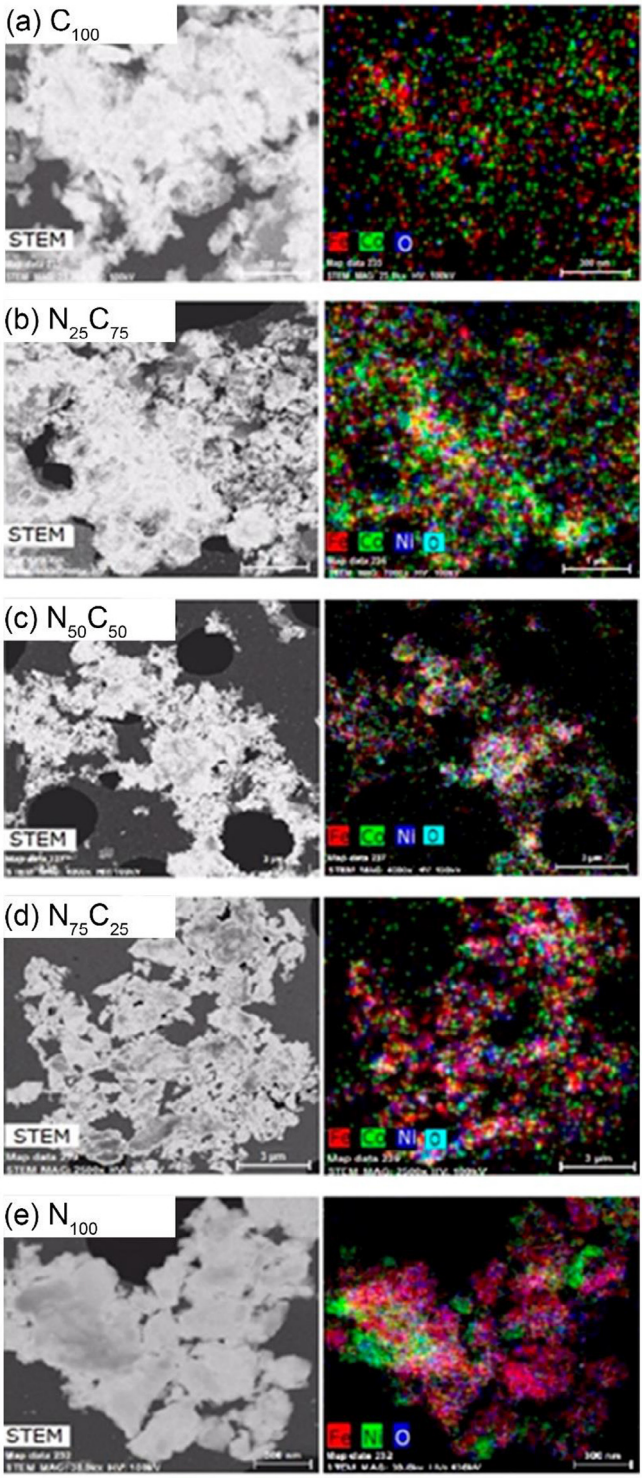

Fig. 2. Elemental map obtained using the STEM-EDX technique. On the left panel pictures of powder with low magnification and in dark-field are presented. The right panel is an elemental distribution of the presented powders, where different colors are attributed to Fe, Co, Ni and O elements.

ferrites (Table 1), because the doped ions occupy the same positions in the spinel, a small deviation of about 0.5° is due to the difference of radii of the Co^{2+} (0.74 Å) and Ni^{2+} (0.72 Å) ions [10]. The average size of crystallites, d_{XRD}, was calculated for the (4 4 0) peaks with Scherrer's formula [27–29]:

$$d_{XRD} = 0.94 \cdot \lambda / (B \cdot cos\vartheta)$$

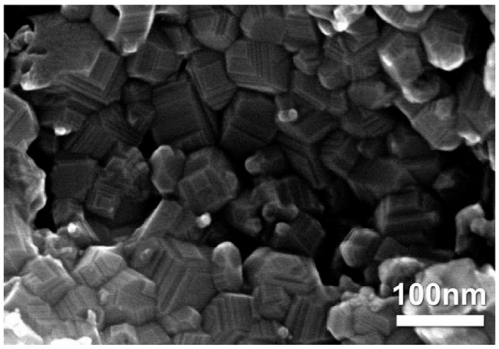

Fig. 3. Bright-field SEM image of $Ni_{0.75}Co_{0.25}Fe_2O_4$ powder. Scale bar is 100 nm.

where B is the full width at half maximum (FWHM) and θ is the position of the XRD peak. The obtained values are in the same order for all samples, however, for Co-Ni ferrites these values of grain size are higher than for pure cobalt and nickel ferrites. This behavior, the increase of particle size with the increase of nickel content and the decrease of particle size for a pure nickel ferrite was observed earlier for Co-Ni ferrites prepared via a hydrothermal route [10]. The XRD-spectra for cobalt ferrite sample and for the sample with the content of nickel less than 0.75 suggests the presence of only one phase of cubic spinel but with the increase of the nickel content, satellite peaks referred to hexagonal hematite and to cubic metallic nickel were observed [30].

Elemental maps of Ni, Co, Fe and O were obtained in a combined STEM-EDX measurement (Fig. 2). The obtained elemental maps show a uniform distribution of the elements in the nanoparticles, which indicates the stoichiometric composition of the particles. Only for the sample of nickel ferrite N_{100}, the regions with a high nickel content were detected, which agrees with the XRD data, which indicate the small presence of metallic nickel in this sample. The particles have a complex irregular shape with distinct cubic faces, as is shown on the SEM image (Fig. 3). A sharp shape confirms the fact that the particles have high crystallinity caused by the high temperature during the growth and crystallization of particles. The particles are in a strongly aggregated state in particular because of the strong dipole–dipole interactions between them.

3.2. Magnetic properties

The room temperature hysteresis loops demonstrate a quasi-static ferrimagnetic behavior for all samples (Fig. 4a). The monotonic shape of the hysteresis loops without any kinks proves the lack of mixtures of soft and hard phases according to a structural study with XRD and STEM-EDX [7]. The monotonic decrease of coercivity with the increase of nickel content from 132 ± 1 mT to 20.5 ± 3 mT for C_{100} and N_{100} samples respectively was observed (Table 2 and Fig. 4b). That is predictable because of the strong single ion anisotropy of the cobalt: indeed the $CoFe_2O_4$ is a hard magnetic material with the bulk magnetic anisotropy constant of $\sim 3 \cdot 10^5$ J/m^3 while the $NiFe_2O_4$ is soft with the magnetic anisotropy constant of $\sim 7 \cdot 10^3$ J/m^3 (values of magnetic anisotropy constants adopted from [31]). These results are in agreement with the switching field distribution (SFD) demonstrated in Fig. 5 obtained as the first derivative of the remanent magnetizations after DCD protocol versus reversal field, dM_{DCD}/dH_{rev}. The set of dM_{DCD}/dH_{rev} curves clearly reflects the soft and hard nature of cobalt and nickel ferrites and the adjustable intermediate anisotropy for mixed ferrites.

The remanent magnetization ratio, M_R/M_S, of about 0.5 suggests that the particles are uniaxial single-domain magnets according to the Stoner–Wohlfarth model [32]. The single-domain state of the particles is consistent with the grain sizes calculated from the XRD and observed on the SEM images, which are less than the critical sizes denoted above. Observed M_R/M_S values suggest the uniaxial anisotropy of the samples

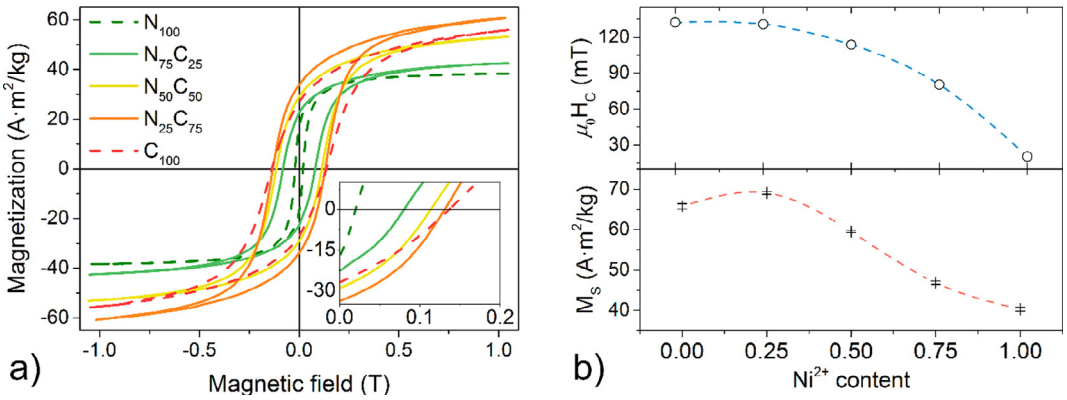

Fig. 4. (a) Hysteresis loops of powders at room temperature. Inset: magnification of the region of coactivity and remanent magnetization; (b) top and bottom panels represent the dependence of coercivity (H_C) and magnetization saturation (M_S) respectively on Ni^{2+} content. Errors for coercivity value are in the range of the symbols.

Table 2
Magnetic properties of powder at room temperature. Uncertainties in the last digit are given in brackets.

Sample	Coercivity μ_0H_C, mT	Switching field μ_0H_{SFD}, mT	Saturation magnetization M_S, A·m²/kg	Remanent ratio M_R/M_S, a.u.	Anisotropy constant Keff, $\times 10^5$ J/m³
C_{100}	132(1)	175(5)	65.8(6)	0.44(4)	1.4(1)
$N_{25}C_{75}$	131(2)	149(5)	69.1(3)	0.49(2)	1.3(1)
$N_{50}C_{50}$	113(2)	132(5)	59.5(3)	0.49(2)	1.5(1)
$N_{75}C_{25}$	80.6(6)	91(4)	46.9(4)	0.54(5)	1.7(1)
N_{100}	20.5(3)	21(1)	40.3(5)	0.43(5)	0.58(7)

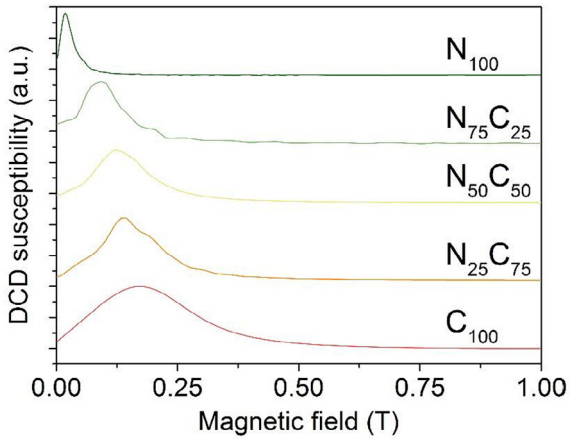

Fig. 5. Switching field distribution of powders at room temperature.

despite the cubic magneto-crystalline anisotropy of the bulk cobalt ferrite, which predicts a value of about 0.8 [33]. This can be explained as interparticle interactions or shape-induced demagnetization effects because of the complicated shapes of the particles [34,35]. The impact of the thermal relaxations on the remanent magnetization is expected to be negligible because of the relatively big volume of the particles.

The SFD correlates with the distribution of particle coercivity fields and, in general, it reflects only irreversible magnetization processes. Positions of SFD maximums, μ_0H_{SFD}, are in good proximity with coercivity field for the pure nickel ferrite sample N_{100}, however, with the decrease of the nickel content it becomes different, as shown in Table 2. Considering the fact that all samples have an identical type of anisotropy and the magnetic interactions are expected to be equal, a possible explanation of the divergence is the forming of domains in highly anisotropic samples as the contribution of the biggest particles in the assembly because of the broadness of the size distribution.

The room temperature saturation magnetization of the samples was estimated using the LAS method explained in the experimental section and the results are presented in Table 2. The sample with the smallest nickel content, $N_{25}C_{75}$, showed a relatively good value of M_S with respect to the sample of pure cobalt ferrite Co_{100}. This phenomenon was observed earlier in the mixed ferrites, but it shows a strong dependence on the synthesis method [20]. The deviation from linear behavior of M_S versus Co^{2+}/Ni^{2+} ratio was attributed to the cation distribution or spin canting effect on the surface, which is more important for fine particles. We expect that further study of samples with low nickel content can lead to important results for further applications. It should be noted that the used method allows producing the magnetic nanoparticles with high values of M_S and H_C without additional processing of powders. This advantage is very important for use in industry, so for example, the particles of the same composition prepared with most commonly used co-precipitation have comparable values of magnetization saturation only after calcination at 600 °C [20].

For nanoparticles with uniaxial anisotropy, the values of effective anisotropy constant (K_{eff}) can be roughly estimated from the anisotropy field μ_0H_K (field value when the hysteresis loop is close):

$$Keff = \mu_0 H_K \cdot M_S/2$$

The calculated values of K_{eff} are reported in Table 2. All values for samples with the cobalt content are in the same range, only the pure nickel powder shows a lower value. Because the K_{eff} values depend slowly on Co^{2+} content, the low influence of magnetocrystalline anisotropy on effective anisotropy can be concluded where the shape anisotropy probably is dominant. This fact does not agree with the earlier results for smaller particles [13], where the influence of the surface and magnetocrystalline anisotropy were predominant. Nevertheless, these values are significantly high even with respect to the bulk material and smaller MNPs at 5 K [13].

4. Conclusions and future perspectives

The presented study reveals magnetic and structural features of the Co-Ni ferrites powders depending on cobalt and nickel ratio. A relative small deviation of the grain size in the range of 17–29 nm was confirmed for mixed ferrites. The predominant presence of the spinel ferrite phase was indicated, however, satellites peaks on the XRD pattern were

detected with the increase of nickel content, which happened because the method initially was adjusted for pure cobalt ferrite MNPs. For future research, the purity of mixed ferrites can be improved, for example, with the variation of concentrations of salts and ratio of salts to citric acid. All samples show relatively high values of M_S and H_C without any thermal treatment. The higher value of magnetization saturation was found for the $Ni_{0.25}Co_{0.75}Fe_2O_4$ sample and approximately equal values of coercivity for $CoFe_2O_4$ and $Ni_{0.25}Co_{0.75}Fe_2O_4$. Notable was the relatively high M_S and H_C values together with the higher electrical resistivity observed elsewhere of nickel ferrite, making a powder with a nickel content of about 0.25 very promising for future the energy applications.

Acknowledgments

The reported study was funded partially by RFBR according to the research project 17-32-50202\17. The discussion of results has been made possible through the mobility grant provided by the 5 top 100 Russian Academic Excellence Project at the Immanuel Kant Baltic Federal University. VR thanks the Ministry of Education and Science of the Russian Federation in the framework of Government assignment 3.9002.2017/6.7.

Conflicts of interest

None.

References

[1] B. Pacakova, S. Kubickova, A. Reznickova, D. Niznansky, J. Vejpravova, Spinel Ferrite Nanoparticles: Correlation of Structure and Magnetism, Magnetic Spinels – Synthesis, Properties and Applications, InTech, 2017.
[2] G. Barrera, et al., Cation distribution effect on static and dynamic magnetic properties of Co1-xZnxFe2O4ferrite powders, J. Magn. Magn. Mater. 456 (2018) 372–380.
[3] M. Pardavi-Horvath, Microwave applications of soft ferrites, J. Magn. Magn. Mater. 216 (2000) 171–183.
[4] R. Valenzuela, Novel, applications of ferrites, Phys. Res. Int. 2012 (2012).
[5] D. Sander, et al., The 2017 Magnetism Roadmap, J. Phys. D Appl. Phys. 50 (2017) 363001.
[6] I.C. Nlebedim, A.J. Moses, D.C. Jiles, Non-stoichiometric cobalt ferrite, CoxFe3 − xO4 (x = 1.0 to 2.0): Structural, magnetic and magnetoelastic properties, J. Magn. Magn. Mater. 343 (2013) 49–54.
[7] V. Mameli, et al., Studying the effect of Zn-substitution on the magnetic and hyperthermic properties of cobalt ferrite nanoparticles, Nanoscale 8 (19) (2016) 10124–10137.
[8] B.D. Cullity, C.D. Graham, Introduction to magnetic materials, Mater. Today 12 (3) (Mar. 2009) 45.
[9] U. Lüders, et al., $NiFe_2O_4$: a versatile spinel material brings new opportunities for spintronics, Adv. Mater. 18 (13) (2006) 1733–1736.
[10] H.Y. He, Structural and magnetic property of Co1-xNixFe$_2$O$_4$ nanoparticles synthesized by hydrothermal method, Int. J. Appl. Ceram. Technol. 11 (4) (2013) 1–11.
[11] K.M. Srinivasamurthy, et al., Tuning of ferrimagnetic nature and hyperfine interaction of Ni2 + doped cobalt ferrite nanoparticles for power transformer applications, Ceram. Int. (2018).
[12] S. Joshi, M. Kumar, Effect of Ni2 + substitution on structural, magnetic, dielectric and optical properties of mixed spinel $CoFe_2O_4$ nanoparticles, Ceram. Int. 42 (16) (2016) 18154–18165.
[13] G. Muscas, et al., Evolution of the magnetic structure with chemical composition in spinel iron oxide nanoparticles, Nanoscale 7 (32) (2015) 13576–13585.
[14] D. Peddis, et al., Spin-canting and magnetic anisotropy in ultrasmall $CoFe_2O_4$ nanoparticles, J. Phys. Chem. B 112 (29) (2008) 8507–8513.
[15] J. Parmar, K. Villa, D. Vilela, S. Sánchez, Platinum-free cobalt ferrite based micromotors for antibiotic removal, Appl. Mater. Today 9 (2017) 605–611.
[16] S.L. Viñas, et al., Tuning the magnetism of ferrite nanoparticles, J. Magn. Magn. Mater. 415 (2016) 20–23.
[17] I. Sharifi, H. Shokrollahi, S. Amiri, Ferrite-based magnetic nanofluids used in hyperthermia applications, J. Magn. Magn. Mater. 324 (6) (2012) 903–915.
[18] A. Sutka, G. Mezinskis, Sol-gel auto-combustion synthesis of spinel-type ferrite nanomaterials, Front. Mater. Sci. 6 (2) (2012) 128–141.
[19] K. Maaz, W. Khalid, A. Mumtaz, S.K. Hasanain, J. Liu, J.L. Duan, Magnetic characterization of Co1 − xNixFe2O4 (0⩽x⩽1) nanoparticles prepared by co-precipitation route, Phys. E Low-dimensional Syst. Nanostructures 41 (4) (2009) 593–599.
[20] B. Ryu, et al., Preparation of Co1-xNixFe2O4 nanoparticles by coprecipitation method, Phys. status solidi 201 (8) (2004) 1855–1858.
[21] J. Utomo, A.K. Agustina, E. Suharyadi, T. Kato, S. Iwata, Effect of Co concentration on crystal structures and magnetic properties of Ni 1–x Co x Fe 2O4 nanoparticles synthesized by co-precipitation method, Integr. Ferroelectr. 187 (1) (Feb. 2018) 194–202.
[22] Y. Tang, X. Wang, Q. Zhang, Y. Li, H. Wang, Solvothermal synthesis of Co1-xNixFe2O4 nanoparticles and its application progress in natural science : materials International solvothermal synthesis of Co 1 À x Ni x Fe 2 O 4 nanoparticles and its application in ammonia vapors detection, Prog. Nat. Sci. Mater. Int. 22 (1) (2012) 53–58.
[23] I. Sharifi, Magnetic and structural studies on $CoFe_2O_4$ nanoparticles synthesized by co-precipitation, normal micelles and reverse micelles methods, J. Magn. Magn. Mater. 324 (10) (2012) 1854–1861.
[24] S. Jovanović, M. Spreitzer, M. Otoničar, J.-H. Jeon, D. Suvorov, pH control of magnetic properties in precipitation-hydrothermal-derived $CoFe_2O_4$, J. Alloys Compd. 589 (Mar. 2014) 271–277.
[25] C. Cannas, A. Falqui, A. Musinu, D. Peddis, G. Piccaluga, $CoFe_2O_4$ nanocrystalline powders prepared by citrate-gel methods: Synthesis, structure and magnetic properties, J. Nanoparticle Res. 8 (2) (2006) 255–267.
[26] G. Bertotti, Hysteresis in magnetism, Hysteresis Magn. (1998) 3–30.
[27] N. Daffé, et al., Magnetic anisotropies and cationic distribution in $CoFe_2O_4$nanoparticles prepared by co-precipitation route: Influence of particle size and stoichiometry, J. Magn. Magn. Mater. 460 (2018) 243–252.
[28] U. Holzwarth, N. Gibson, The Scherrer equation versus the ' Debye – Scherrer equation', Nat. Nanotechnol. 6 (9) (2011) 534.
[29] H.G. Jiang, M. Rühle, E.J. Lavernia, On the applicability of the x-ray diffraction line profile analysis in extracting grain size and microstrain in nanocrystalline materials, J. Mater. Res. 14 (02) (1999) 549–559.
[30] R.T. Downs, M. Hall-Wallace, The American Mineralogist crystal structure database, Am. Mineral. 88 (1) (2003) 247–250.
[31] K.M. Krishnan, Fundamentals and Applications of Magnetic Materials, Oxford University Press, 2016.
[32] E.C. Stoner, E.P. Wohlfarth, "A Mechanism of Magnetic Hysteresis in Heterogeneous Alloys", *Philos. Trans. R*, Soc. A Math. Phys. Eng. Sci. 240 (826) (1948) 599–642.
[33] J. Geshev, A.D.C. Viegas, J.E. Schmidt, Negative remanent magnetization of fine particles with competing cubic and uniaxial anisotropies, J. Appl. Phys. 84 (3) (1998) 1488–1492.
[34] A. López-Ortega, E. Lottini, C.D.J. Fernández, C. Sangregorio, Exploring the magnetic properties of cobalt-ferrite nanoparticles for the development of a rare-earth-free permanent magnet, Chem. Mater. 27 (11) (Jun. 2015) 4048–4056.
[35] D. Peddis, F. Orrù, A. Ardu, C. Cannas, A. Musinu, G. Piccaluga, Interparticle interactions and magnetic anisotropy in cobalt ferrite nanoparticles: influence of molecular coating, Chem. Mater. 24 (6) (2012) 1062–1071.